[1]Tengxu Xia

Real-time Gait Event Tracker (RGET): An Innovative Approach to Digital Human Modeling through Integration of Inertial Measurement Unit and Dynamic Feature Extraction

Journal of Electrical Systems

Abstract: - The advancement of digital human modeling technology underscores the importance of accurately representing human characteristics and behaviors using motion capture technologies. This paper introduces the Real-time Gait Event Tracker (RGET), an advanced method aimed at precisely detecting gait events via an Inertial Measurement Unit (IMU), thereby supporting high-precision digital human modeling. RGET integrates planning techniques into continuous states and action spaces, utilizing first-order difference functions and sliding window techniques to effectively identify four key gait events: Heel Strike (HS), Toe Off (TO), Walking Start (WS), and Walking Pause (WP). The system efficiently manages IMU gait signal data through real-time queuing techniques and extracts dynamic features within time frames using positive/negative windowed first-order difference integrations. By adopting weighted sleep time methods and adaptive threshold decision rules, RGET accurately extracts gait event features from sequences. Not only does RGET support precise gait segmentation with an F1 score of 95.9%, but it also provides an innovative method for digital human modeling and its applications.

Keyword: Digital Human Modeling; Motion Capture Technology; Gait Event Detection; Inertial Measurement Unit; Dynamic Feature Extraction, Design and Ergonomics; Biomechanics; Wearable Technology.

I. INTRODUCTION

In the interdisciplinary fields of Mathematics [1], Engineering [2], and Computer Sciences [3], as well as basic and biological sciences, the significance of gait analysis is increasingly recognized, particularly in its application to wearable technologies [4] and human-robot interaction [5]. Gait analysis, a sophisticated method for assessing human locomotion [6], is pivotal in the development of exoskeletons and other human-interactive robotic systems.

In the specialized area of wearable exoskeleton systems, the importance of precise control [7] and sophisticated behavior perception [8] cannot be overstated. A critical aspect of this control system is the use of Euler angle data [9], which is primarily obtained through accelerometers [10] and gyroscopes [11]. These sensors play a fundamental role in the lower limb sensing of exoskeleton robots, enabling the precise depiction of the lower limbs' orientation in three-dimensional space.

The efficient and real-time processing of Euler angle data is essential for exoskeleton robots to determine their orientation and position accurately. This capability is crucial for refining the control of their movements, especially in critical aspects such as posture control [12], strategic motion planning [13], structural design [14] and environmental adaptability [15]. Moreover, the integration of sensor data is vital for fault diagnosis [16] and the development of effective feedback mechanisms [15,17,18] within these robotic systems.

In the sphere of gait-centric robotic systems, including exoskeleton robots, the phases of "Gait Initiation" [19,20] and "Gait Termination" [21,22] are key in understanding user intentions. The phase of "Gait Initiation" signals the moment a user begins walking [23]. Accurately detecting this moment is crucial for activating the exoskeleton's assistive motion modalities [24], aligning the robot's support [25] with the user's intended walking pattern [26]. On the other hand, "Gait Termination" indicates the end of a walking sequence [27]. Recognizing this event enables the exoskeleton to reduce or stop support [28], allowing for a natural and safe conclusion to the user's movement.

In the detailed study of the gait cycle, the events of Toe-Off (TO) [29,30] and Heel Strike (HS) [31,32] hold paramount importance, as shown in Figure 1. TO marks the beginning of the swing phase and is characterized by the moment the toe leaves the ground at the end of a walking cycle [33]. This event is crucial for facilitating stabilization and preparing for the swing phase. On the other hand, HS signifies the start of the stance phase,

[1] Haide College, Ocean University of China
* Corresponding Author: Tengxu Xia

occurring when the heel makes its initial contact with the ground [34]. This phase is essential for providing stability and reducing impact forces during the support phase of walking. The exoskeleton system, by responding to these events, can offer crucial propulsive assistance for the subsequent step, thereby enhancing the overall efficiency of walking.

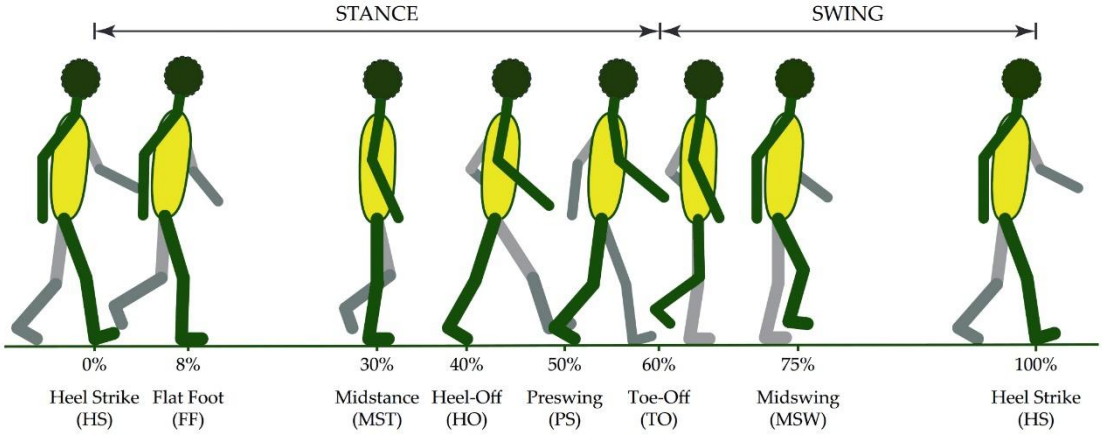

Figure 1: Phases of the Human Gait Cycle. This diagram represents the progression of a single gait cycle, highlighting the transitions between major events such as Heel Strike (HS), Flat Foot (FF), Midstance (MST), Heel-Off (HO), Preswing (PS), Toe-Off (TO), Midswing (MSW), and returning to Heel Strike (HS). Each phase is annotated with its approximate percentage duration of the total gait cycle.

Therefore, the accurate identification and response to these four fundamental gait events—Heel Strike (HS), Toe-Off (TO), Walking Start (WS), and Walking Pause (WP)—from continuous data is critical in achieving synchronization between the robot and the user's natural gait rhythm. This synchronization is key to enhancing walking efficacy [11], comfort [35], and the safety [36] of the robot's application.

However, the precise detection [37] and analysis [38] of these gait events remain a significant challenge, especially in dynamic and variable environments [39,40], as shown in Figure 2. One of the primary difficulties lies in differentiating actual gait events like toe-off from incidental movements [41] such as foot jittering [42]. Traditional methods of gait analysis often struggle to discern these subtle but critical differences, especially across varied gait patterns and in different environmental contexts. For instance, the amplitude and frequency of foot motion can change with variations in step frequency and pace during different activities like walking or running, adding complexity to the task of accurate gait event detection. This complexity underscores the need for advanced techniques in gait analysis, capable of effectively navigating and interpreting these nuanced aspects of human movement within the context of exoskeleton technology.

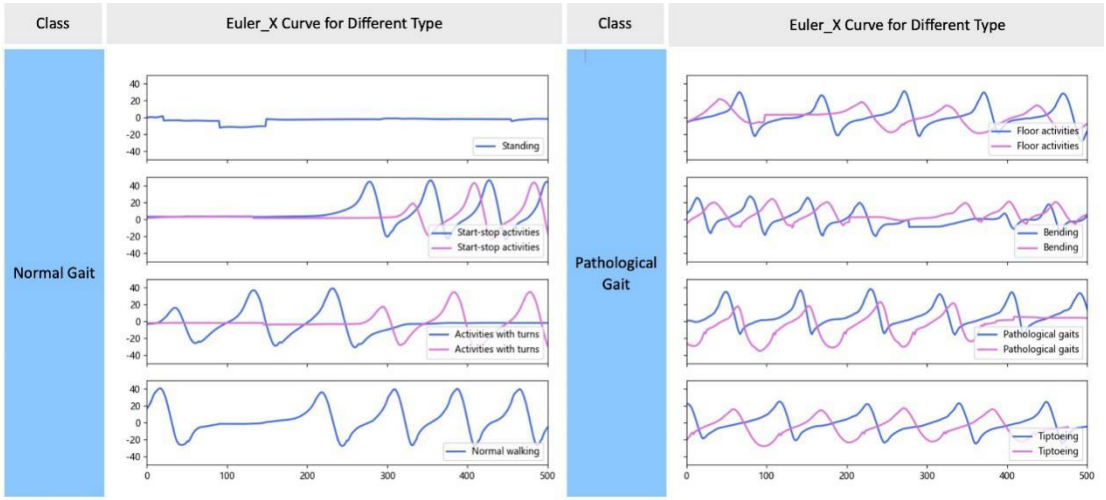

Figure 2: Examples of gait Euler Angle pulse curves in different scenarios. (a) is the gait curve of standing still; (b) to (e) are the gait curves of normal walking; (f) to (l) show the pathological gait curves.

The task of accurately interpreting peaks within gait data [43] is a significant challenge in real-world gait analysis. Identifying a peak that signifies a toe-off event is just the first step; the algorithm must also be judicious in not misinterpreting closely spaced peaks as consecutive toe-off events, which are unlikely within a normal gait cycle. This necessitates a mechanism within the algorithm to "suspend" its activity temporarily. Such a suspension prevents the misidentification of nearby peaks as separate events, thereby reducing the likelihood of false alarms caused by noise.

Another major challenge is the precise recognition and adjustment to variations in gait curve amplitudes under different conditions [44,45]. Traditional gait analysis methods often employ fixed thresholds to detect events like toe-off or heel strike. However, this approach generally lacks the flexibility needed to accommodate changes in gait under varying conditions. For example, a transition from a slow walk to a sprint or moving across different terrains can result in shifts in gait speed and pattern. In such scenarios, fixed thresholds may not adequately capture all crucial gait events.

Furthermore, variations in gait curves are influenced by individual differences [46], the intensity of activities [47], and environmental factors [48]. These create intertwined challenges that call for a comprehensive approach. Activities with varying intensities, such as high-speed movements, typically produce higher amplitudes and more frequent events, while gentler activities result in lower amplitudes and frequencies. Discrepancies in amplitude and frequency across different activity intensities can lead to inaccuracies in detecting gait events.

Therefore, a method that is adaptable and comprehensive is essential to effectively navigate these complex fluctuations and challenges. This method should be capable of dynamically adjusting to varying gait conditions, accurately interpreting the data, and discerning true gait events from noise and other non-gait movements. By addressing these complexities, advancements in gait analysis can lead to more accurate and reliable control of exoskeleton systems, improving their efficacy and user experience.

In response to these intricate challenges, our research introduces a series of innovative methodologies. We have engineered an advanced gait detection system specifically for complex settings, named the Real-time Gait Event Tracker (RGET). This system utilizes Euler angle data from the lower limbs of exoskeleton robots to achieve high-precision, multi-event detection in real time. The RGET method enhances the precision in pinpointing vital gait events and is specially designed to adapt to dynamic and variable conditions. It demonstrates exceptional sensitivity and versatility in recognizing a range of gait patterns.

Furthermore, our study incorporates a novel approach called the weighted sleep time strategy. This strategy significantly improves the accuracy and adaptability of gait event detection. It does so by dynamically altering the algorithm's sensitivity and its period of inactivity, or "sleep," thereby reducing the likelihood of false detections due to closely spaced or erroneous peaks.

Additionally, we have developed an adaptive threshold decision mechanism. This approach continuously adjusts detection thresholds to suit individual walking patterns and changes in the environment. It does this by calculating a weighted average of the detected pulse peaks and setting this average as the new benchmark for peak identification. This method allows the system to respond effectively to variations in gait speed, intensity, and environmental factors.

The primary contributions of our research are manifold, offering significant advancements in the realm of gait analysis:

This article makes several contributions to the field of human activity intention recognition:

- Advanced High-Precision Multi-Event Real-Time Gait Detection Method: Our research introduces a groundbreaking method for gait detection, particularly suited for complex environments. This method stands out for its high precision and capability to handle multiple gait events simultaneously in real-time. It excels not only in increasing the accuracy of identifying critical gait events but also demonstrates remarkable applicability and flexibility across various dynamic and fluctuating scenarios.
- Novel Weighted Sleep Time Strategy: We have innovated a weighted sleep time strategy that revolutionizes the way gait event detection algorithms operate. By dynamically adjusting the algorithm's sensitivity and its inactive periods, this strategy substantially boosts the accuracy and flexibility in detecting gait events. This approach effectively mitigates the risk of false positives and enhances the algorithm's ability to respond to true gait events accurately, even in complex situations.
- Cutting-Edge Adaptive Threshold Decision Rule: Our research has yielded an adaptive threshold decision rule, specifically designed for real-time adaptation of detection thresholds in response to varying gait events. This rule is adept at accommodating shifts in the amplitude of gait curves that occur in different scenarios, such as changes in walking speed or terrain.

II. MATERIALS AND METHODS

The Real-time Gait Event Tracker (RGET) algorithm, a sophisticated tool in our research arsenal, is founded on the principles of time series analysis and signal processing. This algorithm utilizes real-time differential and integral operations to precisely identify characteristic features within the gait time series data. Such an approach is crucial for pinpointing key gait events, particularly from limited local data

Rooted in dynamic systems theory, the RGET algorithm's core strategy revolves around discerning and interpreting patterns and trends from continuous data streams. As illustrated in our figures 3, this algorithm comprises several integral components: a time-window slope differentiation function, an innovative adaptive threshold decision rule, and a uniquely developed weighted sleep time method.

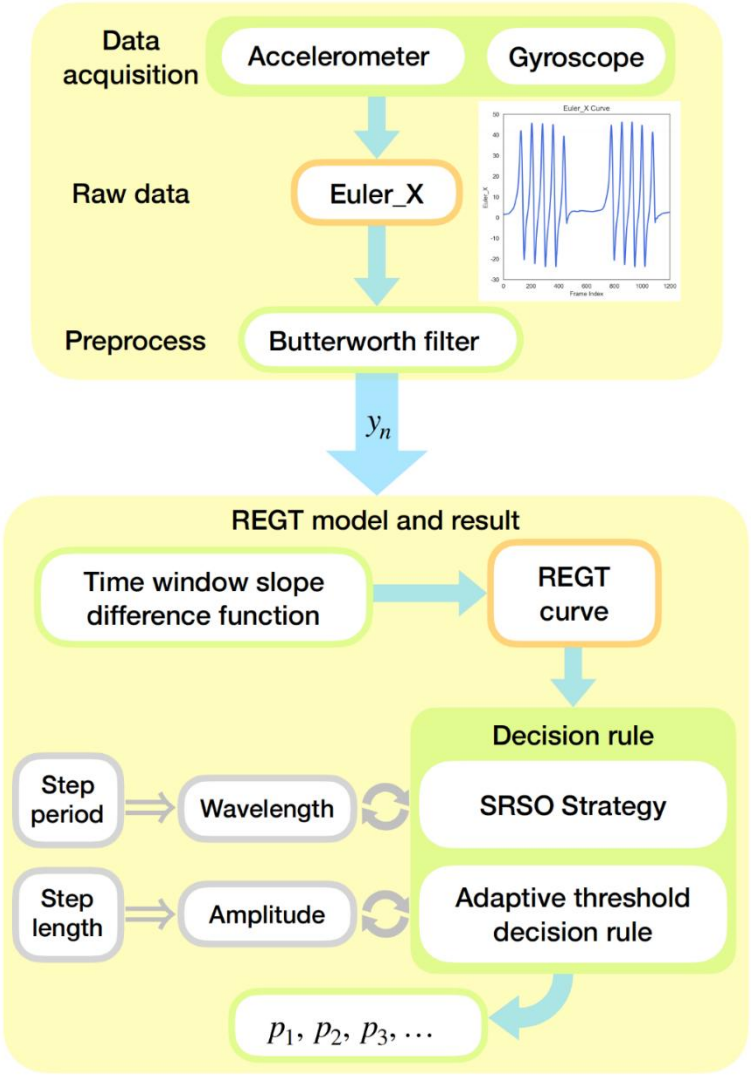

Figures 3: Overview of the Recursive Gait Event Timing (RGET) Algorithm Framework. This flowchart delineates the step-by-step process employed by the RGET algorithm, starting from data acquisition using accelerometers and gyroscopes, through preprocessing with a Butterworth filter, to the analysis using a time-window slope difference function and the execution of the adaptive threshold decision rule.

The time-window slope differentiation function is engineered to analyze the slope changes within a specific time window, enabling the algorithm to detect subtle variations in gait patterns. The adaptive threshold decision rule is designed to dynamically adjust the detection thresholds, accommodating changes in gait amplitude and frequency. This ensures the algorithm remains sensitive and accurate under varying conditions. Lastly, the weighted sleep time method plays a pivotal role in enhancing the algorithm's precision. It intelligently modulates the algorithm's sensitivity and inactive periods, preventing false detections and ensuring the algorithm reacts accurately to true gait events.

A. Real-time Gait Event Tracker

The Real-time Gait Event Tracker (RGET) algorithm is meticulously designed to focus on local amplitude variations within gait data, a crucial aspect for identifying specific events in the gait cycle, such as Heel Strike (HS) and Toe Off (TO). The primary aim of RGET is to accurately trace the rising and falling slopes of the gait curve, a process achieved through sequential frame analysis within a dynamically shifting time window. This analysis leads to the creation of what we refer to as the RGET curve, a refined representation of the gait cycle's key features.

In order to elucidate the workings of the proposed Relative Gradient Echo Tracking (RGET) method, Figure 3 presents a comparative analysis between pulse data, difference signals, positive RGET, and negative RGET. The top panel of the figure displays the pulse data waveform, which is indicative of the initial signal captured by the system.

"The 'difference' signal displayed in the second panel of Figure 4 is derived from the first-order difference of the Pulse Data, representing the rate of change or the gradient of the pulse waveform at each point. the 'difference' curve, illustrated with a blue line, incorporates areas filled in green and red, which signify the integral of the increment changes within a specific window compared to a baseline signal. The green-filled areas represent regions where the integral is greater than zero, corresponding to positive slope changes in the gait data. Conversely, the red-filled areas represent regions where the integral is less than zero, corresponding to negative slope changes.

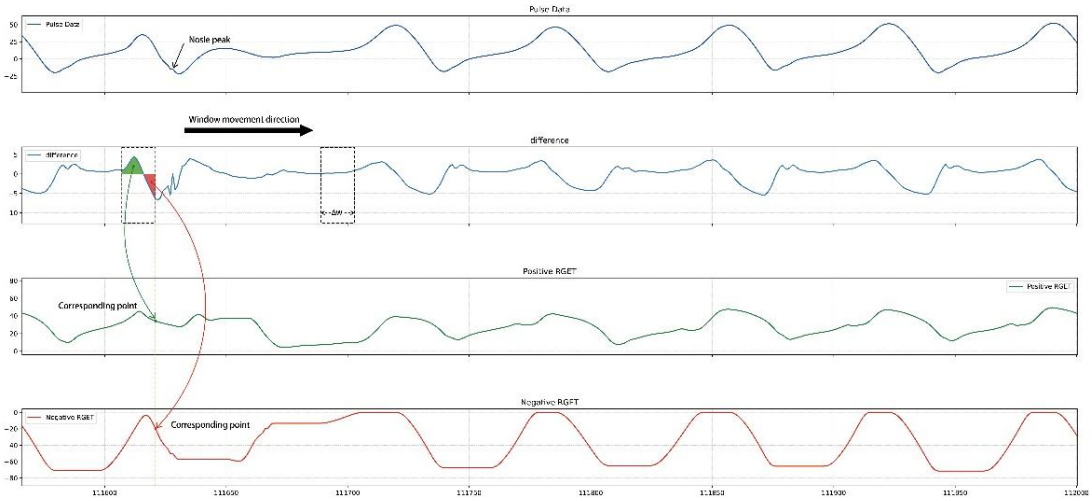

Figure 4: Examples of gait curves processed using RGET, depicting the relationship between pulse data, differential signals, and the RGET outputs. The topmost graph showcases the 'Pulse Data' with identifiable peaks, which represents the raw signals obtained from the gait analysis. The difference signal is derived from the first-order difference of the Pulse Data, representing the rate of change or the gradient of the pulse waveform at each point. The subsequent panels illustrate 'Positive RGET' and 'Negative RGET' signals, which accumulate these positive and negative differences respectively, offering a clear visualization of the gait cycle's upward and downward trends.

This first-order differential is crucial as it accentuates the instantaneous changes in the Pulse Data, enabling the detection of subtle variations that might be indicative of significant events within the signal. By computing the first-order difference, we highlight the velocity of the signal's change rather than its absolute values. Peaks in the 'difference' signal correspond to rapid increases in the Pulse Data, while troughs correspond to rapid decreases.

This differential approach allows the RGET algorithm to be sensitive to the dynamics of the signal, providing a powerful tool for detecting transient events that could be lost if only the raw data were considered. The ability

to detect these dynamic changes underpins the RGET method's capability to accurately track and analyze complex time-series data in real-time."

To enhance its effectiveness in detecting the peaks and troughs that characterize the gait curve, the RGET algorithm integrates two specialized methodologies: GSFSpos and GSFSneg. Each of these methodologies has a distinct focus and operational definition, tailored to address specific aspects of the gait cycle:

a) RGETpos (Positive Real-time Gait Event Tracker)

This component of the RGET algorithm concentrates on identifying positive slope variations within the gait data. It is specifically engineered to detect the ascending phases of the gait curve, which are indicative of certain key gait events. By isolating and analyzing these positive slopes, GSFSpos aids in accurately pinpointing moments like the initial phase of Heel Strike or the early stages of Toe Off. Its expression is given in Eq.1.

$$\boldsymbol{RGET_{pos}} = \sum_{\boldsymbol{k=i-w}}^{\boldsymbol{i}} \boldsymbol{\Delta u_k}, \boldsymbol{\Delta u_k} = \begin{cases} \boldsymbol{0}: \boldsymbol{\Delta u_k} \leq \boldsymbol{0} \\ \boldsymbol{\Delta u_k}: \boldsymbol{\Delta u_k} > \boldsymbol{0} \end{cases} \quad (1)$$

Where ω specifies the duration of the time window, y_k indicates the Euler angle measurements of the gait curve. The difference signal, denoted as Δuk in the equation 1, represents the incremental changes in the gait data. It is calculated by taking the difference between consecutive Euler angle measurements $\Delta y_k = y_k - y_{k-1}$. This difference is only considered when there is an increase in the angle value $\Delta y_k > 0$, which corresponds to the positive slope variations in the gait curve. When the change is non-positive $\Delta y_k \leq 0$, the 'difference' is set to zero, as the focus is solely on the ascending phases of the gait curve.

The RGETpos is a sum of these 'difference' signals over a specified time window ω. This summation process enhances the detection of positive gradient changes within the gait data. In practical terms, RGETpos is sensitive to the initiation and progression of upward trends in the gait cycle, such as the initial phase of a Heel Strike or the onset of a Toe Off. This sensitivity allows RGETpos to serve as a reliable indicator for the commencement of key gait events, facilitating their precise detection in real-time applications.

By isolating and accumulating positive increments within the time window, the RGETpos forms a curve that can precede the actual peaks in the gait curve. This characteristic is crucial for real-time event detection, as it enables the identification of gait events slightly before they reach their maximal value, ensuring timely and responsive tracking of the gait cycle.

b) RGETneg(Negative Real-time Gait Event Tracker)

In contrast, GSFSneg is designed to focus on the negative slope variations in the gait data. This methodology is essential for recognizing the descending phases of the gait curve. By scrutinizing these negative slopes, GSFSneg plays a critical role in identifying other crucial points in the gait cycle, such as the completion of Toe Off or the latter phase of Heel Strike. Its expression is given in Eq.2.

$$\boldsymbol{RGET_{neg}} = \sum_{\boldsymbol{k=i-w}}^{\boldsymbol{i}} \boldsymbol{\Delta u_k}, \boldsymbol{\Delta u_k} = \begin{cases} \boldsymbol{0}: \boldsymbol{\Delta u_k} \leq \boldsymbol{0} \\ \boldsymbol{\Delta u_k}: \boldsymbol{\Delta u_k} > \boldsymbol{0} \end{cases} \quad (2)$$

Where ω specifies the duration of the time window, $\Delta y_k = y_k - y_{k-1}$ indicates the Euler angle measurements of the gait curve. Similarly, the Negative RGET, represented by the red curve, aggregates all negative 'difference' signals, occurring when $\Delta y_k = y_k - y_{k-1} \leq 0$, which indicates a downward trend in the gait cycle. Hence, when the gait curve shows a decreasing slope, the Negative RGET sums these decrements, forming a trough in the graph, which precisely signals the conclusion of gait events, like the completion phase of Toe Off.

Together, GSFSpos and GSFSneg enable the RGET algorithm to conduct a comprehensive and nuanced analysis of the gait curve. Vertical lines marked as 'Corresponding point' serve to align significant points on the pulse data with those on the Positive and Negative RGET curves. This alignment elucidates how these elements are interrelated and provides a clear visual guide for understanding the dynamic interactions within the gait cycle. This dual approach ensures that all critical phases of the gait cycle are accurately identified, allowing for a more precise and holistic understanding of human locomotion.

B. Dynamic rule update

In the realm of practical gait analysis, the formation of pulse peaks unfolds in two distinct scenarios: those instigated by Toe Off events and those emanating from disruptive factors like foot tremors. Drawing a clear distinction between these scenarios is paramount, as only the former provides reliable data for accurate gait prediction. Once pulse peaks are identified, the crucial step lies in implementing decision rules that translate the extracted gait curve features into meaningful gait events. These rules encapsulate three pivotal aspects:

1) Alternating Occurrences of Peaks: Within the continuous gait curve, the anticipation of alternating instances of peaks is a fundamental expectation. Typically, each gait cycle encompasses a single occurrence of both Heel Strike (HS) and Toe Off (TO) events, and the algorithm recognizes this alternation pattern.

2) Temporal Gap between Identical Gait Events: The natural pace of walking dictates a temporal gap between identical gait events. This temporal criterion serves as a vital tool in distinguishing authentic peaks induced by Toe Off from those arising due to foot tremors. Following the identification of a Toe Off-induced peak, the algorithm strategically enters a "sleep" phase. During this temporary hiatus, the detection of new peaks is momentarily halted. This strategic approach aligns with the principles of human gait biomechanics, acknowledging the improbability of two Toe Off events occurring within a standard gait cycle.

3) Threshold Baseline for Extreme Values: Peaks and troughs associated with TO and HS events in both the gait and RGET curves typically represent the cycle's maximal or minimal values. To filter out extreme values, an initial threshold baseline is set at 60\% of the adjacent curve's amplitude. Only peaks and troughs emerging beyond this baseline in both the gait curve signal and RGET signal are deemed valid for detection. This meticulous thresholding ensures precision and relevance in the gait analysis process.

However, achieving a delicate balance between real-time precision and accuracy in the application of the second and third rules poses substantial challenges, especially in dynamic and variable environments. Diverse gait contexts introduce unique curve features such as amplitude, period, and phase shifts, rendering static thresholds and sleep durations less effective in these multifaceted real-world scenarios. To address these challenges, our research introduces a synergistic approach that combines highly adaptive thresholds with a weighted sleep time methodology. This dual strategy is meticulously designed to adeptly navigate the intricacies of dynamic and multifarious gait environments, ensuring unparalleled accuracy and responsiveness in gait analysis.

a) Step-Responsive Sleep Optimization (SRSO) Strategy

To implement this innovative approach, we have devised a weighted queue system that dynamically adjusts sleep durations based on the current characteristics of gait data. The adaptive sleep interval is finely tuned to the individual's step frequency and speed, adapting to different walking contexts. For instance, in scenarios involving rapid walking, the sleep duration is shortened to align with the increased stepping rates. Conversely, during slow-paced walking, the sleep interval is prolonged to minimize the impact of noise. Data is selectively admitted into the pulse peak window queue only when it aligns with predefined time intervals specific to the gait scenario. This method serves the dual purpose of filtering out noise while ensuring the precise capture of crucial gait events. The mathematical formulation of the Step-Responsive Sleep Optimization Strategy is outlined as Eq.3:

$$\mathrm{T}_{\mathrm{gap}} = \frac{\sum_{i=1}^{q_{\mathrm{len}}} RT_i w_i}{\sum_{i=1}^{q_{\mathrm{len}}} w_i} \tag{3}$$

In our model, we define a peak time window queue denoted as q, where $\mathrm{RT_i}$ represents the minimal sleep duration for the n^{th} significant peak. The length of the queue is indicated by q_{len}, and RT_i denotes the sleep duration recorded at the i^{th} position within q. Additionally, w_i illustrates the weight assigned to the i^{th} position in the queue. Our framework posits that weights are more substantial closer to the queue's entrance. Therefore, as one progresses from the queue exit to the entrance, w_i incrementally increases from 1 to q_{len}. This sophisticated formulation ensures a dynamic and adaptive sleep time strategy that aligns with the evolving characteristics of gait data, enhancing the accuracy and responsiveness of the overall system in diverse and dynamic gait scenarios.

b) Adjustive Bar Decision Rule

In addressing the dynamic amplitude alterations observed in gait curves across diverse scenarios, our research introduces an innovative adaptive threshold decision rule. This rule is meticulously crafted for the real-time recalibration of the detection threshold for pulse peaks, thereby enhancing the accuracy and adaptability of peak identification.

Built on a simple yet effective observation, the adaptive threshold decision rule acknowledges the inherent variability in gait curve amplitudes across different scenarios. Activities characterized by rapidity or intensity often result in more pronounced amplitudes, contrasting with the subdued amplitudes observed in slower or more moderate activities. Consequently, relying on a static threshold for pulse peak detection proves insufficient in accommodating the entire spectrum of scenarios. The algorithm requires a dynamic modulation of the pulse peak detection threshold in real-time, accommodating the variability in individual gait patterns and environmental dynamics.

To address this challenge, our research devises a dynamic threshold computation mechanism that actively monitors pulse peaks within each position of the weighted queue. For every emerging pulse peak, its threshold is established as 60% of the aggregated weighted average of existing pulse peaks within the queue. This criterion ensures that a new pulse peak is recognized as valid and allowed entry into the pulse peak queue only if it exceeds this dynamically adjusted threshold. The baseline threshold for pulse peaks is denoted as Threshold_0. In cases where $n-1$ peaks have already been validated and incorporated into the peak time window queue, the adaptive threshold for the subsequent, or n^{th}, peak is determined by the following Eq4:

$$\text{Bar}_n = \frac{k\sum_{i=1}^{q_{\text{len}}} \text{P}_i w_i}{\sum_{i=1}^{q_{\text{len}}} w_i} \tag{4}$$

Here, Threshold_n represents the threshold for the n^{th} validated peak, while P_i denotes the peak value at position i within the queue q. This formulation is integral to our dynamic threshold computation mechanism, ensuring the precision of peak validation in the analysis of gait data.

C. Evaluation Indicator

To rigorously evaluate the performance of our model under various configurations, we employ four pivotal metrics: Detection Rate, True Negative Rate (TNR), False Positive Rate (FPR), and the F1-Score. Each metric offers a distinct perspective on the predictive capabilities of our model, thus facilitating a comprehensive assessment of its accuracy and reliability.

a) Detection Rate

The Detection Rate quantifies the model's proficiency in identifying positive instances, calculated as the ratio of correctly identified positive instances to the total number of positive instances present. Formally, it is expressed as:

$$\text{Detection Rate} = \frac{\text{TP}}{\text{TP+FN}} \tag{5}$$

where TP denotes True Positives and FN denotes False Negatives. A high Detection Rate signifies the model's effectiveness in capturing positive samples, crucial for applications demanding high sensitivity in positive class identification.

b) True Negative Rate (TNR)

The True Negative Rate (TNR), also known as Specificity, measures the model's ability to accurately identify negative instances. It is the proportion of correctly predicted negative instances to the total actual negative instances, defined as:

$$\text{TNR} = \frac{\text{TN}}{\text{TN+FP}} \tag{6}$$

where TN represents True Negatives and FP represents False Positives. TNR is particularly vital when dealing with imbalanced datasets, as it helps discern whether the model merely favors the majority class or genuinely distinguishes between classes.

c) False Positive Rate (FPR)

The False Positive Rate (FPR) is the converse of TNR, representing the proportion of negative instances incorrectly labeled as positive, relative to the total number of actual negative instances:

$$\text{FPR} = \frac{\text{FP}}{\text{TN+FP}} \tag{7}$$

Reducing the FPR is paramount in applications where misclassifying negative instances as positive could have grave consequences, making it a critical metric for evaluating model performance.

d) F1-Score

The F1-Score is the harmonic mean of Precision and Recall, offering a singular metric that balances both precision and recall. It is especially relevant for imbalanced datasets, as it concurrently considers both the accuracy and completeness of the positive class predictions:

$$\text{F1-Score} = 2 \times \frac{\text{Precision} \times \text{Recall}}{\text{Precision+Recall}} \tag{8}$$

In this study, we further explore the impact of two critical hyperparameters—Sleeptime and bar—on these evaluation metrics to identify the optimal model configuration. Through this analytical approach, we aim to provide a nuanced understanding of the model's performance, particularly in complex or imbalanced data scenarios.

III. EXPERIMENT

A. Data Preparation and Experimental Setup

In this exploratory study, we recruited four healthy male subjects, each devoid of notable physical or cognitive impairments that could potentially influence their gait patterns. Participants were equipped with a singular Inertial Measurement Unit (IMU), securely positioned on the anterior section of the tibia using an adjustable nylon buckle strap. The IMU maintained seamless connectivity with a handheld device via Bluetooth, enabling data transmission at a frequency of 60Hz. Positioned precisely along the longitudinal axis of the tibia, the IMU underwent calibration to accurately capture the tibial angular velocity in the sagittal plane, with a primary focus on the x-axis.

In a comprehensive exploration of the dynamic spectrum of human gait, our study specifically targeted two principal gait modalities: natural and pathological. Natural gait involved extended periods of consistent ambulation interspersed with phases of rest, encompassing rapid transitional movements, turns, and static standing phases. The primary objective for the algorithm was to attain optimal stability and precision. In contrast, pathological gait was characterized by increased tremors and erratic fluctuations in frequency and amplitude. Data acquisition spanned across these diverse states, capturing transitions from stillness to motion and vice versa for each participant. The extensive dataset comprised approximately 1,500 individual gait samples, encompassing various walking patterns such as regular walking, rapid transitions, turning, standing, shuffling, and specific pathological gaits simulating movements seen in Parkinsonian conditions.

The IMU gathered crucial data, including tibial angular velocity, acceleration, and step timing, with gait events (Heel Strike, Toe Off, Walking Start, Walking Pause) meticulously annotated through video assessment and non-real-time processing. Additionally, all data compilation was conducted within a controlled environment, utilizing splicing techniques for real-time algorithmic detection. This approach simulated authentic scenarios of varied walking patterns interspersed with stationary periods, ensuring the fidelity and dependability of our findings.

B. Hyperparameter optimization and adaptive parameter range determination

In the process of optimizing model performance, selecting appropriate evaluation metrics and adjusting model hyperparameters are crucial. In this study, we utilized Detection Rate, True Negative Rate (TNR), False Positive Rate (FPR), and F1 Score as evaluation metrics with the aim of optimizing model performance by adjusting the hyperparameters Sleep time and Bar.

The objective of hyperparameter optimization in this research was to find the optimal values of Sleep time and Bar that maximize the model's detection rate and TNR, while achieving the highest possible F1 Score and maintaining a low FPR. To achieve this goal, we employed a systematic optimization strategy, namely, analyzing the impact of hyperparameters on evaluation metrics through two-dimensional and three-dimensional relationship graphs.

a) Optimal selection of Detection Rate

Initially, we collected a series of model performance data under various Sleep time and Bar through experiments. The experimental design adhered to strict variable control principles, ensuring one hyperparameter was varied while the other remained constant. This process involved extensive model training and evaluation to ensure the reliability and validity of the data.

The Figure 5 (a) illustrating the Detection Rate as a function of Sleep Count values for both gait events HS and TO reveals an initially high Detection Rate across lower values. The Detection Rate for the HS event remains relatively stable up to a Sleep Count of about 40, suggesting that this range is suitable for optimizing detection. At the same time, the Detection Rate for the TO event starts to decline sharply after a Sleep Count value near 40. Consequently, an optimal Sleep Count value for the TO event would be below 40 to achieve the best Detection Rate.

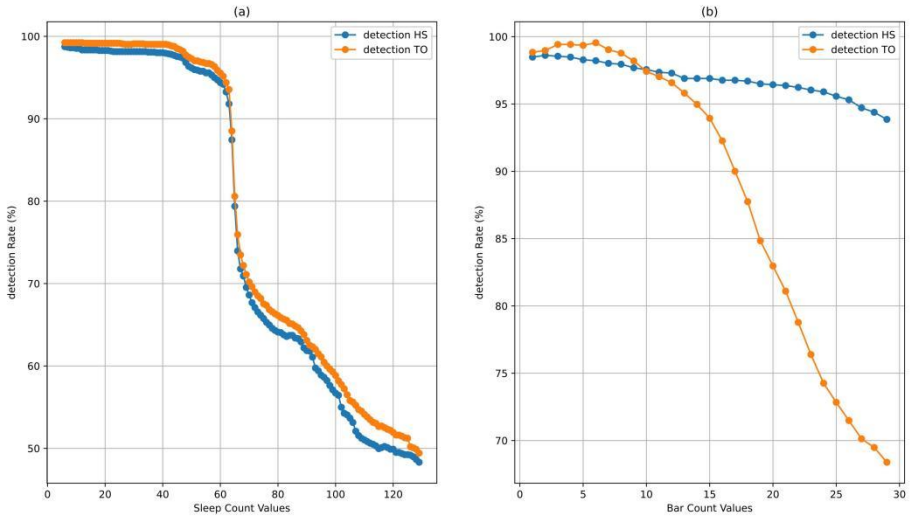

Figure 5: Impact of Sleep Count and Bar on Detection Rate for Gait Events HS and TO

The Figure 5 (b) that plots Detection Rate against Bar Count values reveals nuanced behaviors for the gait events HS and TO. The HS event displays a marginal decline in Detection Rate with increasing Bar Count values, suggesting a minimal impact on detection performance and implying robustness across the tested range. This slight decrease indicates that while there is some sensitivity to the Bar Count parameter, its effect does not substantially compromise the HS event's Detection Rate.

Conversely, the Detection Rate for the TO event remains significantly high at Bar Count values below 10, emphasizing its effective detection capability within this range. Notably, the TO event Detection Rate peaks at a Bar Count of 6, where it achieves its optimal performance. Maintaining the Bar Count at or near 6 for the TO event appears to be particularly conducive to achieving a high Detection Rate, highlighting the importance of this value for the TO detection optimization.

b) Optimal selection of TNR

Analyzing the two-dimensional plots of Figure 6 provided for the True Negative Rate (TNR) in relation to the Sleep Count and Bar Count values, we observe distinct trends for the TNR of the gait events High Sensitivity (HS) and Threshold Optimization (TO).

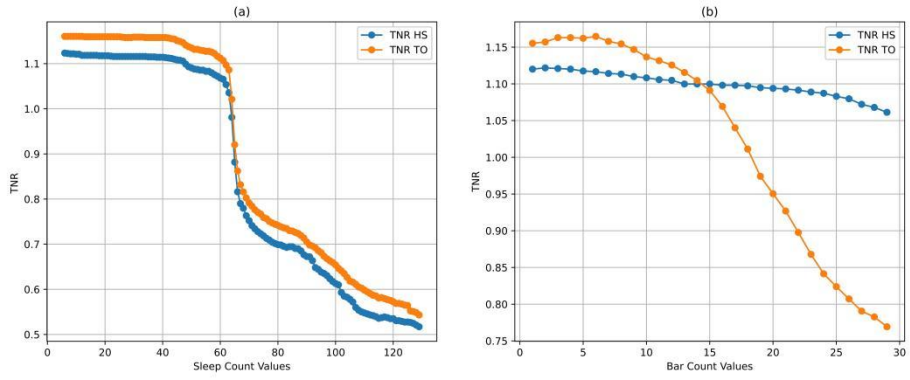

Figure 6: Impact of Sleep Count and Bar on TNR for Gait Events HS and TO

Figure 6 (a) demonstrates the relationship between TNR and Sleep Count values for the gait events High Sensitivity (HS) and Threshold Optimization (TO). The TNR for both events initially shows stability, underscoring the models' capabilities in correctly identifying true negative cases at lower Sleep Count values. HS maintains a high TNR up to a Sleep Count of approximately 40, indicating that within this range, the model has a lower likelihood of falsely detecting an event when there is none. The slight decline beyond this point suggests a marginal decrease in specificity, which may not significantly affect the model's overall performance, but it is still a consideration for setting an upper limit on the Sleep Count value. TO, on the other hand, exhibits a marked

decrease in TNR past a Sleep Count value of 44, suggesting a critical threshold for maintaining high specificity. Thus, Sleep Count values less than 44 are recommended for optimal specificity in both HS and TO events.

In Figure 6 (b), the pattern of TNR with respect to Bar Count values reveals a peak performance zone for HS, indicating a range where the system is most adept at avoiding false negatives. The observed peak for HS, between Bar Count values of 3 to 8, represents the optimal balance between sensitivity and specificity. This is where the system is neither overly conservative nor too permissive, which aligns with the principal aim of maintaining a high TNR. In contrast, TO exhibits a high specificity at low Bar Count values, with a sharp decrease beyond the value of 9. For TO, staying below this threshold ensures that true negatives are not mistaken as positives.

c) Optimal selection of FPR

From Figure 7 (a), both HS and TO show a low FPR at smaller Sleep Count values, indicating few false alarms and suggesting a high specificity in this range. The FPR begins to rise sharply after a certain threshold; for HS, this rise starts after a Sleep Count value of approximately 47, while for TO, the increase begins slightly earlier. This rapid increase in FPR beyond these values indicates a decline in the model's specificity, leading to more false positives being identified.

In Figure 7 (b), the FPR for HS remains relatively flat and low across a broader range of Bar Count values, which is indicative of consistent specificity. TO shows a low FPR, up to about 6 column meter values, more than 10 will rise sharply. This suggests that the specificity for TO dramatically decreases as the Bar Count increases, thereby increasing the likelihood of false positives.

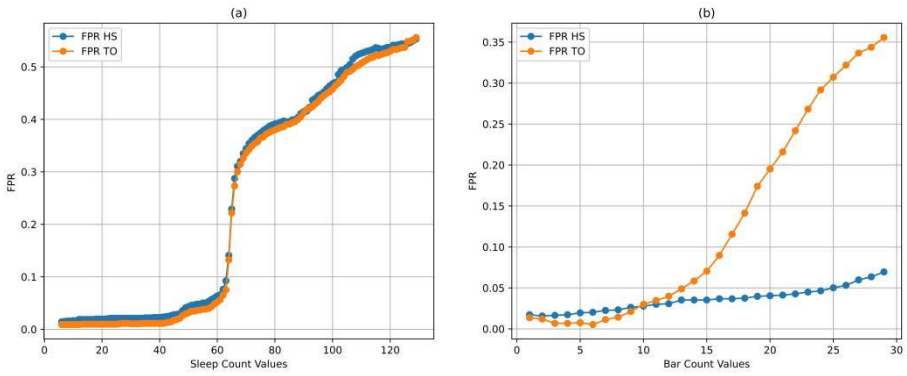

Figure 7: Impact of Sleep Count and Bar on FPR for Gait Events HS and TO

d) Optimal selection of F1 Score

The F1 Score is a critical metric for evaluating model performance, especially in applications where both precision (the model's ability to identify only relevant instances) and recall (the model's ability to identify all relevant instances) are important. In the context of gait event detection, a high F1 Score signifies that the system effectively discriminates between true events and non-events, reducing the likelihood of false identifications and missed detections.

Figure 8 (a) depicts the F1 Score against Sleep Count values. Initially, for lower Sleep Count values, both HS and TO maintain high F1 Scores, indicating a balanced performance between precision and recall. The F1 Score for HS starts to decline after a Sleep Count value of around 62, whereas for TO, the score begins to decrease more significantly beyond this point. This suggests that the predictive performance of TO is more sensitive to changes in Sleep Count than HS.

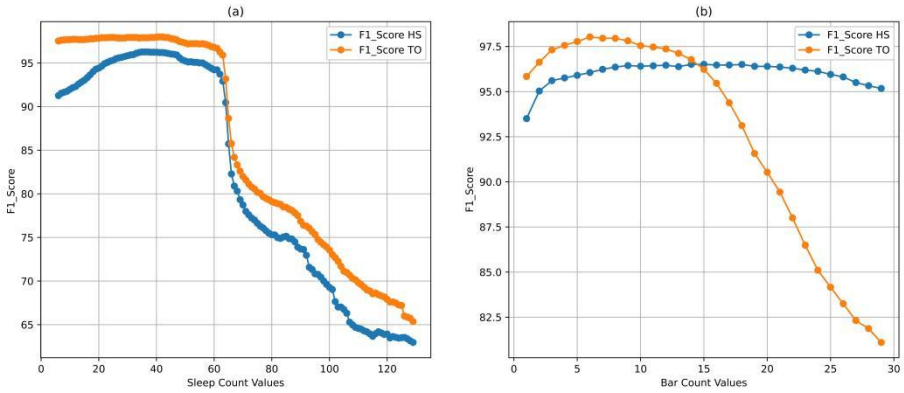

Figure 8: Impact of Sleep Count and Bar on F1-Score for Gait Events HS and TO

In Figure 8 (b), the F1 Score is plotted against Bar Count values. For HS, the F1 Score peaks at a mid-range of Bar Count values and then begins a gradual decline, suggesting that there is an optimal range of Bar Count values that maximizes the balance between false positives and false negatives. In contrast, the F1 Score for TO sharply decreases after a Bar Count value of 15, indicating that its optimal predictive balance is maintained within a narrow range of lower Bar Count values.

e) Assessing the Independence of Hyperparameter

In this section, we delve into the three-dimensional representations that articulate the relationships between two critical hyperparameters—Sleep Count and Bar Count—and four pivotal evaluation metrics: F1 Score, Detection Rate, True Negative Rate (TNR), and False Positive Rate (FPR). Figure 9 provide a comprehensive perspective on how the alterations in hyperparameters influence the model's performance in gait detection tasks.

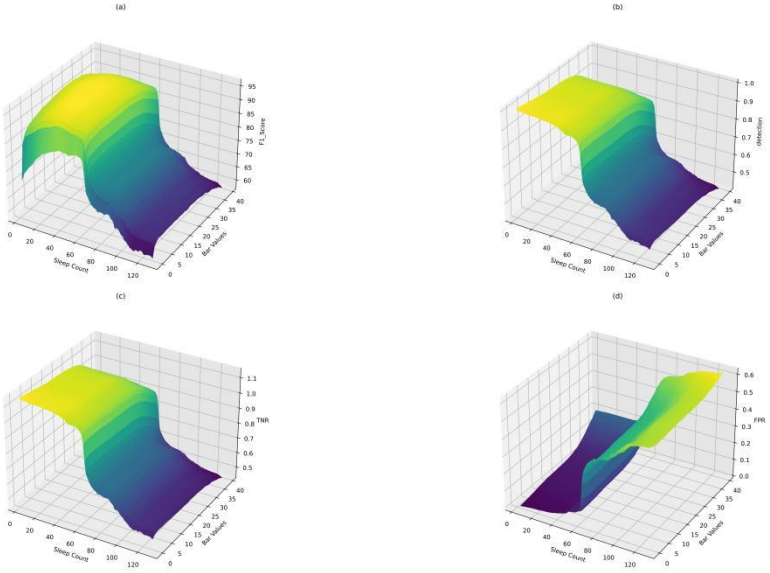

Figure 9: Coupling analysis of hyperparameter and performance index

The Figure 9 (a) showcases a landscape where the optimal regions are represented by peaks that correspond to high F1 Scores. This metric combines precision and recall, hence a high F1 Score suggests a balanced trade-off between these two. The plot illustrates that for both High Sensitivity (HS) and Threshold Optimization (TO) events, there exists a combination of Sleep Count and Bar Count that maximizes the F1 Score, with a discernible ridge that delineates the transition from suboptimal to optimal values.

The Figure 9 (b) illustrates the model's sensitivity—the rate at which true positives are correctly identified. The visualization indicates that within certain ranges of Sleep Count and Bar Count, the Detection Rate reaches a plateau, suggesting a threshold beyond which increasing Sleep Count or Bar Count does not significantly enhance detection capabilities.

The Figure 9 (c) indicates the model's specificity, where higher values correspond to better performance in correctly labeling negatives. The plot demonstrates a clear decline in TNR with increasing Sleep Count and Bar Count, illustrating the model's tendency to incorrectly classify negatives as positives at higher parameter values.

The Figure 9 (d) of the FDR, thus, clearly demarcates the areas of optimal hyperparameter settings. The 'valley'—where the surface is at its lowest—represents the combination of Sleep Count and Bar Count that minimizes the FDR, which is paramount for the practical deployment of a gait event detection system. Within this valley, the model achieves a desirable balance, effectively reducing the occurrence of false positives while maintaining a high detection rate.

Critically, the analyses of Figure 9 suggest a lack of coupling between the evaluation metrics. Each metric evolve independently in response to the hyperparameters. For instance, the F1 Score and Detection Rate do not show direct trade-offs; regions exist where both can be optimized. Similarly, the TNR and FPR plots, while inversely related, do not imply a direct trade-off between them across all ranges of Sleep Count and Bar Count. Instead, they indicate that an optimal balance can be struck, wherein both specificity and the minimization of false positives can be achieved simultaneously. Decoupling of evaluation metrics means that we are able to fine-tune model parameters to achieve specific performance results.

The individual analysis of hyperparameters reveals that:

- Sleep count has a critical impact on all four metrics. When [36,44] is reached, the F1 score and detection rate maintain high values. It shows that both precise recall balance and sensitivity are preserved over this range.
- Bar Count shows a more subtle effect. Although the detection rate remains stable within [4,10], both TNR and F1 scores show sensitivity beyond 9, and in particular the F1 score peaks before decreasing. Therefore, the optimal range of Bar Count is [4,9], where the tradeoff between false positives and false negatives is the most favorable.

C. Ablation Study for SRSO and Adjustive Bar Decision Rule

To rigorously evaluate the significance of SRSO and Adjustive Bar Decision Rule in our gait event detection model, we conducted a series of ablation studies. These experiments were designed to systematically remove or vary these hyperparameters to assess their impact on the model's F1 Score. This approach allows us to isolate the contribution of each hyperparameter to the overall effectiveness of the model.

a) Ablation of SRSO Strategy

The SRSO Strategy is an intricate part of our model that dynamically adjusts the sleep count based on detected step patterns and timing, intending to optimize the sleep duration to the step frequency. To understand the extent of its impact, we first disabled the SRSO Strategy, reverting to a non-responsive, static sleep count set at the previously determined optimal static value.

The ablation results of the SRSO strategy are shown in Figure 10. Without the SRSO Strategy, the model suffered a degradation in performance, primarily evidenced by a decline in the F1 Score. This was particularly noticeable in varying walking speeds, suggesting that the SRSO's dynamic adjustment is vital for maintaining high model performance across different gait dynamics. The ability to adapt the sleep count in real-time is a key factor in ensuring the model's robustness against variability in step patterns.

b) Ablation of Adjustive Bar Decision Rule

Next, we targeted the Adjustive Bar Decision Rule, which dynamically calibrates the bar count to adapt the detection threshold based on recent gait event frequencies. By maintaining the bar count to 0, we analyzed the consequences on the model's precision and false-positive rates.

As shown in Figure 11, the model experienced a significant loss in precision and an uptick in false-positive rates without the Adjustive Bar Decision Rule. The fixed bar count failed to discern subtle variations in gait events as effectively as the dynamic rule, leading to a higher rate of incorrect event classifications. The Adjustive Bar Decision Rule proved to be a critical feature for enhancing the model's discriminative capabilities, enabling a more nuanced detection of genuine gait events.

c) Combined Ablation

The combined ablation of both the SRSO Strategy and Adjustive Bar Decision Rule provided insights into their synergistic operation. As shown in Figure 12, eliminating both features resulted in a further compromised model performance, reinforcing the idea that these features work in tandem to optimize F1 Score.

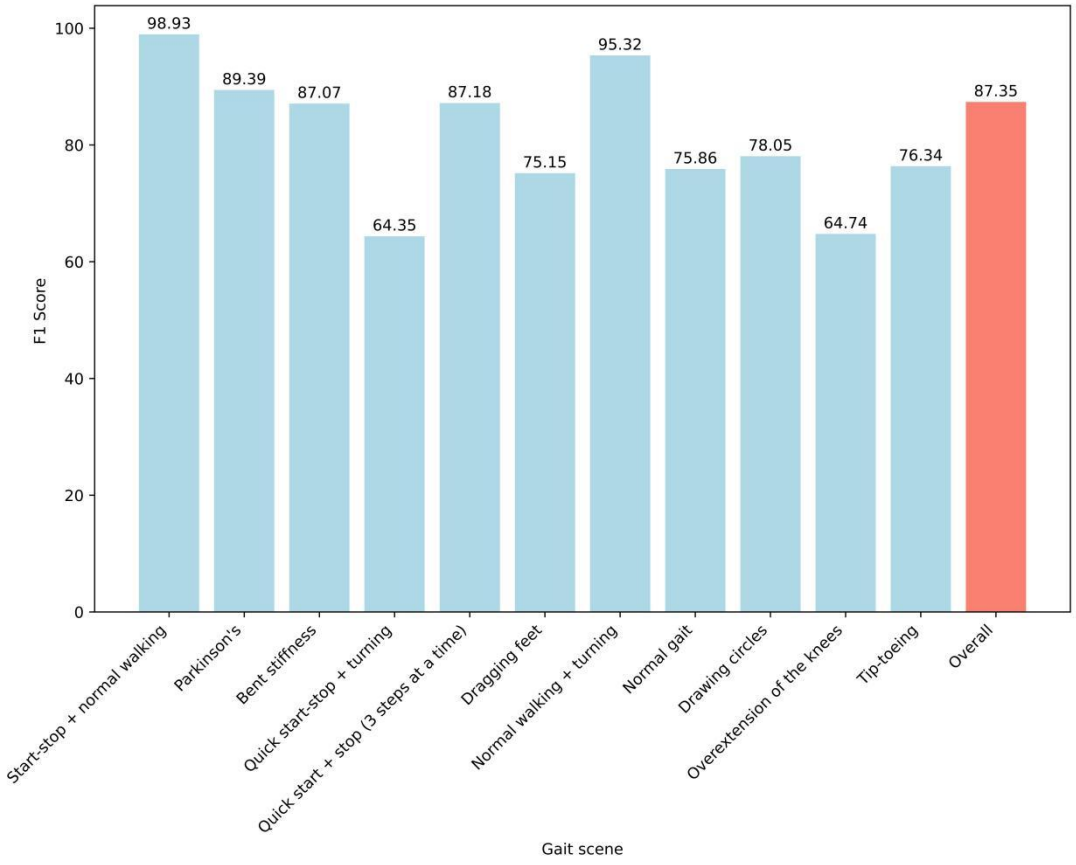

Figure 10: Ablation experiments without SRSO Strategy in various gait scenarios

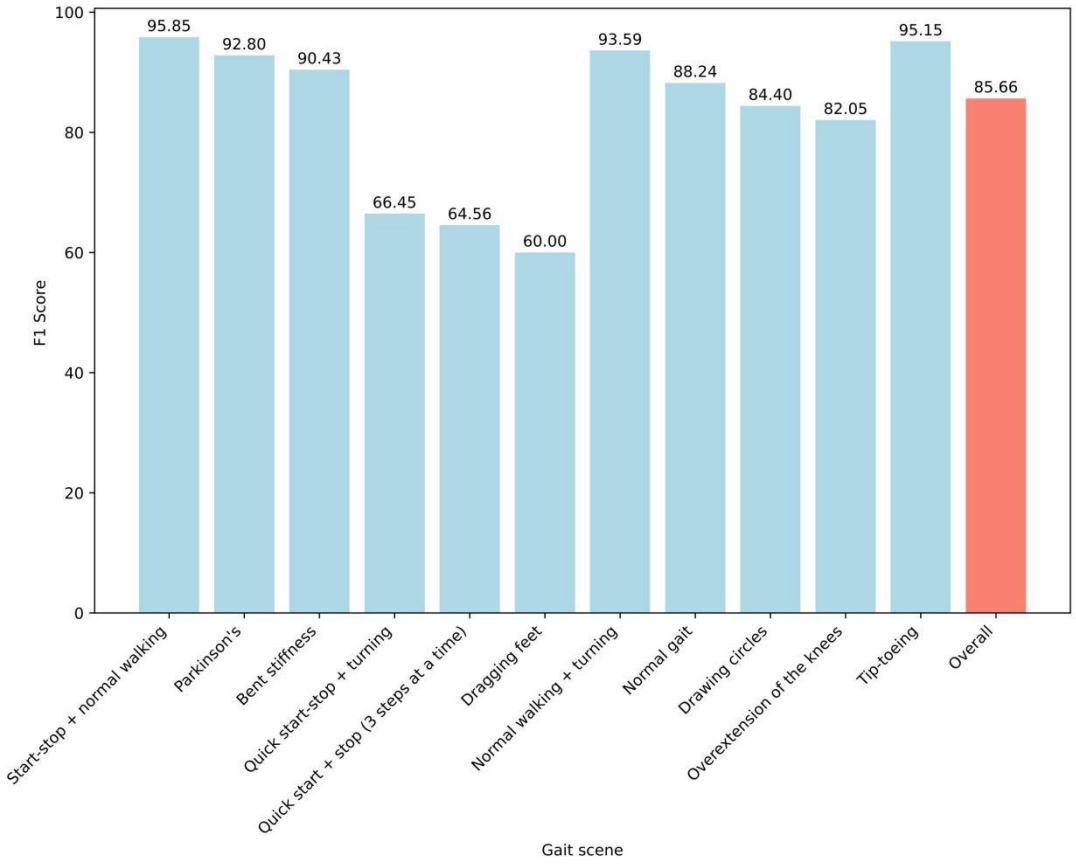

Figure 11: Ablation experiments without adjustive bar decision rule in various gait scenarios

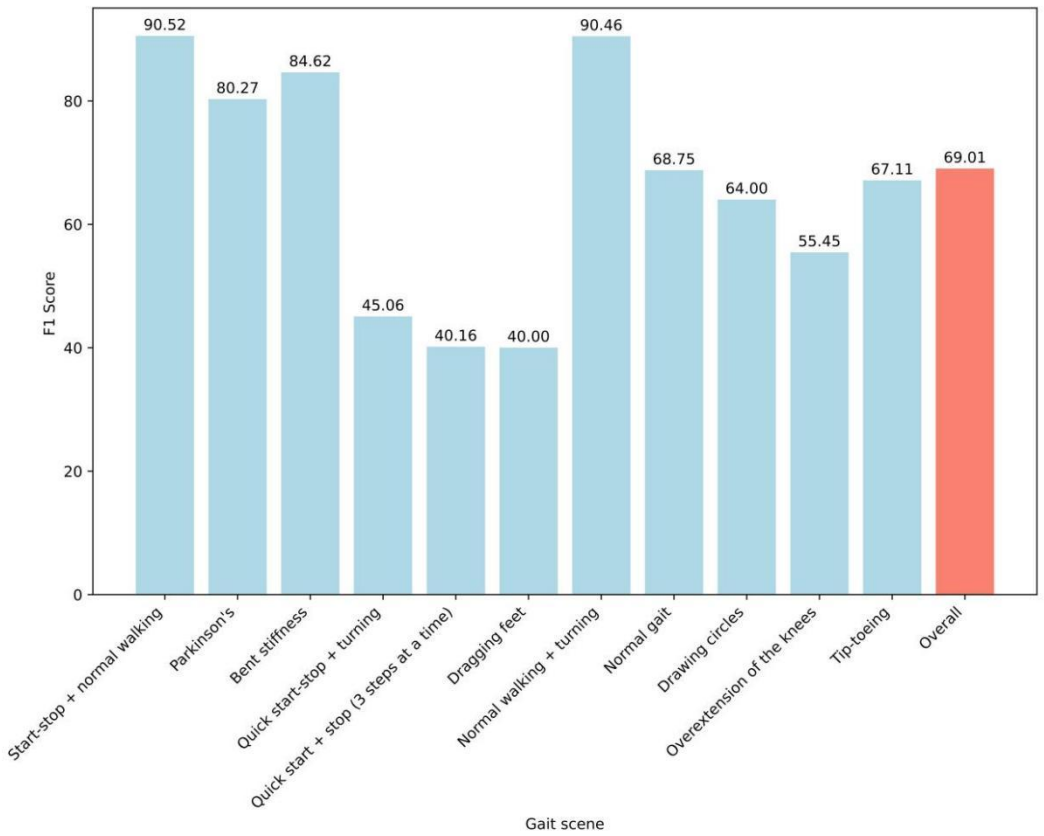

Figure 12: Ablation experiments without SRSO Strategy and adjustive bar decision rule in various gait scenarios

d) Analysis of Ablation Results

From the Table 1 the following observations and analyses can be drawn:

Table 1: Comparison of ablation results for F1 scores in different gait scenarios

Gait Scene	Baseline	Baseline+SRSO	Baseline+Bar Decision	Baseline+SRSO+ Bar Decision
Start-stop+ normal walking	90.25	98.93	95.85	99.64
Parkinson's	80.27	89.39	92.80	96.67
Bent stiffness	84.62	87.07	90.43	97.25
Quick start-stop + turning	45.06	64.35	66.45	87.55
Quick start + stop (3 steps at a time)	40.16	87.18	64.56	94.44
Dragging feet	40.00	75.15	60.00	80.88
Normal walking + turning	90.46	95.32	93.59	97.22
Normal gait	68.75	75.86	88.24	96.88
Drawing circles	64.00	78.05	84.40	97.92
Overextension of the knees	55.45	64.74	82.05	92.59
Tip-toeing	67.11	76.34	95.15	98.99
Overall	69.01	87.35	85.66	95.90

- Start-Stop + Normal Walking: The implementation of SRSO brings about a significant enhancement in F1 score, indicating its effectiveness in dynamic walking patterns. Adding both SRSO and the Bar Decision rule leads to the highest F1 score, which shows that the synergy between responsiveness to step variation and adaptability in decision threshold is particularly beneficial.
- Parkinson's and Bent Stiffness Scenarios: In these scenarios, characterized by irregular and stiff movements, the SRSO strategy alone shows a considerable improvement, suggesting its utility in detecting nuanced gait abnormalities. However, the Adjustive Bar Decision rule alone demonstrates a greater improvement in the Parkinson's scenario, possibly due to its impact on enhancing detection sensitivity. The combined strategies again yield the best F1 scores, underscoring their complementary strengths.

- Quick Start-Stop + Turning and Quick Start + Stop: Scenarios involving rapid changes in movement display a marked improvement with the introduction of SRSO, which effectively adjusts to the abrupt changes in step patterns. The combined application of SRSO and the Bar Decision rule results in a drastic improvement, emphasizing the necessity of adaptive strategies in complex gait patterns.
- Dragging Feet and Overextension of the Knees: These scenarios, which typically involve more subtle gait deviations, benefit from the individual and combined enhancements. However, the combined strategy does not outperform the Bar Decision rule as much in the dragging feet scenario, indicating that while adaptiveness is crucial, the decision rule plays a more significant role in such nuanced cases.
- Normal Walking + Turning and Drawing Circles: These represent scenarios with a mix of predictable and unpredictable movements. The SRSO's incremental improvement suggests its utility in handling regular gait, while the Bar Decision rule's larger impact implies its effectiveness in managing unpredictability. Together, they achieve the highest F1 scores. Tip-Toeing: This unique gait scenario sees one of the largest improvements with the Bar Decision rule, which suggests that adjusting the decision threshold is particularly important for detecting this type of gait.

The Baseline+SRSO configuration consistently improves the F1 scores across all scenarios compared to the baseline, validating the efficacy of the SRSO strategy in enhancing the model's responsiveness to diverse gait patterns.

The Baseline+Bar Decision configuration, while generally effective, particularly shines in scenarios that perhaps involve more consistent gait abnormalities (like Parkinson's), indicating the rule's importance in adjusting the detection threshold sensitively.

The Baseline+SRSO+Bar Decision configuration provides the highest F1 scores in almost all scenarios, underscoring the combined strategies' comprehensive impact on the model's performance. This indicates that while each strategy is effective on its own, their combination provides a synergistic effect that greatly enhances the model's predictive accuracy.

The Overall F1 score indicates a clear hierarchy in performance, with the combined configuration outperforming the individual strategy augmentations, which in turn outperform the baseline. This reveals a cumulative benefit from each strategy, where their integration leads to superior performance compared to their isolated applications.

IV. Conclusion and Future work

The study has successfully developed the Real-time Gait Event Tracker (RGET) algorithm, showcasing its efficacy in precise real-time detection of key gait events across diverse gait patterns. Emphasizing accuracy and adaptability in dynamic environments, the RGET algorithm has demonstrated high performance in scenarios like normal walking, Parkinsonian gait, and flexed stiff gait, maintaining accuracy even in dynamic situations like "rapid initiation + turning." The incorporation of weighted sleep time and Adjustive Bar Decision Rule enhances the algorithm's ability to handle variations in gait curve amplitudes.

By analyzing IMU data, RGET algorithm can effectively distinguish real gait events from false alarms caused by noise, and its F1 Score can reach 95.9%. Despite the remarkable achievements, limitations still exist, especially in abnormal gait patterns such as "dragging" and "knee hyperextension", where sensitivity is reduced. Future research directions could involve refining the algorithm to address these specific patterns and exploring its applicability across diverse demographics and health conditions for real-world scenarios.

Acknowledgment

Funding: This research was funded by a scholarship provided by Ocean University of China. The scholarship supported various stages of the research, including the design, data collection, analysis, and interpretation processes, as well as the writing of the paper. We express our heartfelt gratitude to Ocean University of China for their generous support. This funding not only offered the financial backing needed to conduct this research but also reflected recognition and encouragement towards our research team and objectives. We commit to continuing our efforts in conducting high-quality scientific research that contributes to society and the scientific community.

Institutional review Board Statement: Not applicable.

Informed Consent Statement: Informed consent was obtained from all subjects involved in the study.

Acknowledgments: I would like to extend my sincere thanks to the editors and reviewers of your journal. Thank you for taking the time out of your busy work to review my submission and provide valuable comments and suggestions. Your professional knowledge and patient guidance have played a vital role in my research work.

Conflicts of Interest: The authors declare no conflicts of interest.

REFERENCES

[1] Liu, Y.; Lu, G.; Chen, J.; Zhu, Q. Exploration of Internal and External Factors of Swimmers' Performance Based on Biofluid Mechanics and Computer Simulation. International Journal of Environmental Research and Public Health 2021, 18. https://doi.org/ 10.3390/ijerph18126471.

[2] Save, O.M.; Das, S.; Carlson, E.; Ahn, J.; Lee, H. Human Gait Entrainment to Soft Robotic Hip Perturbation during Simulated Overground Walking. IEEE Transactions on Neural Systems and Rehabilitation Engineering 2024, pp. 1–1. https://doi.org/10.1109/ TNSRE.2024.3354851.

[3] Xing, L.; Yifan, L.; Xingjun, W. Efficient Gait Trajectory Prediction Method Based on Soft Constraint Weighted Template Matching:Work-in-Progress. In Proceedings of the 2023 International Conference on Hardware/Software Codesign and System Synthesis (CODES+ISSS), 2023, pp. 46–47.

[4] Miao, S.; Chen, L.; Hu, R. Spatial-Temporal Masked Autoencoder for Multi-Device Wearable Human Activity Recognition. Proc. ACM Interact. Mob. Wearable Ubiquitous Technol. 2024, 7. https://doi.org/10.1145/3631415. 693.

[5] Wazwaz, A.; Amin, K.; Semary, N.; Ghanem, T. Dynamic and Distributed Intelligence over Smart Devices, Internet of Things Edges, and Cloud Computing for Human Activity Recognition Using Wearable Sensors. Journal of Sensor and Actuator Networks 2024, 13. https://doi.org/10.3390/jsan13010005.

[6] Zhang, P.; Li, Y.; Zhuang, Y.; Kuang, J.; Niu, X.; Chen, R. Multi-level information fusion with motion constraints: Key to achieve high-precision gait analysis using low-cost inertial sensors. Information Fusion 2023, 89, 603–618. 698.

[7] Vu, H.T.T.; Dong, D.; Cao, H.L.; Verstraten, T.; Lefeber, D.; Vanderborght, B.; Geeroms, J. A review of gait phase detection algorithms for lower limb prostheses. Sensors 2020, 20, 3972.

[8] Knoop, V.; Costenoble, A.; Debain, A.; Bravenboer, B.; Jansen, B.; Scafoglieri, A.; Bautmans, I.; de Hert Paul Jansen Bart, G.B.S.G.B.I.V.D.B.I.P.M.D.D.L.K.T.R.G.C.P.S.A.C.E. Muscle Endurance and Self-Perceived Fatigue Predict Decline in Gait Speed and Activities of Daily Living After 1-Year Follow-Up: Results From the BUTTERFLY Study. The Journals of Gerontology: Series A 2023, 78, 1402–1409.

[9] Fang, Z.; Woodford, S.; Senanayake, D.; Ackland, D. Conversion of Upper-Limb Inertial Measurement Unit Data to Joint Angles: A Systematic Review. Sensors 2023, 23, 6535.

[10] Yoon, D.H.; Kim, J.H.; Lee, K.; Cho, J.S.; Jang, S.H.; Lee, S.U. Inertial measurement unit sensor-based gait analysis in adults and older adults: a cross-sectional study. Gait & Posture 2024, 107, 212–217.

[11] Liu, Y.; Liu, X.; Wang, Z.; Yang, X.; Wang, X. Improving performance of human action intent recognition: Analysis of gait recognition machine learning algorithms and optimal combination with inertial measurement units. Computers in Biology and Medicine 2023, 163, 107192. https://doi.org/https://doi.org/10.1016/j.compbiomed.2023.107192.

[12] Guo, J.; Zhang, Q.; Chai, H.; Li, Y. Obtaining lower-body Euler angle time series in an accurate way using depth camera relying on Optimized Kinect CNN. Measurement 2022, 188, 110461.

[13] Zhou, J.; Ma, H.; Chen, J.; Jia, S.; Tian, S. Motion characteristics and gait planning methods analysis for the walkable lunar lander to optimize the performances of terrain adaptability. Aerospace Science and Technology 2023, 132, 108030.

[14] Kan, K.; Binama, M.; Chen, H.; Zheng, Y.; Zhou, D.; Su, W.; Muhirwa, A. Pump as turbine cavitation performance for both conventional and reverse operating modes: A review. Renewable and Sustainable Energy Reviews 2022, 168, 112786.

[15] Kan, K.; Zhang, Q.; Xu, Z.; Zheng, Y.; Gao, Q.; Shen, L. Energy loss mechanism due to tip leakage flow of axial flow pump as turbine under various operating conditions. Energy 2022, 255, 124532.

[16] Alemayoh, T.T.; Lee, J.H.; Okamoto, S. Leg-Joint Angle Estimation from a Single Inertial Sensor Attached to Various Lower-Body Links during Walking Motion. Applied Sciences 2023, 13, 4794.

[17] Madrigal, J.A.B.; Rodríguez, L.A.C.; Pérez, E.C.; Rodríguez, P.R.H.; Sossa, H. Hip and lower limbs 3D motion tracking using a double-stage data fusion algorithm for IMU/MARG-based wearables sensors. Biomedical Signal Processing and Control 2023, 86, 104938.

[18] Kan, K.; Chen, H.; Zheng, Y.; Zhou, D.; Binama, M.; Dai, J. Transient characteristics during power-off process in a shaft extension tubular pump by using a suitable numerical model. Renewable Energy 2021, 164, 109–121.

[19] Zhao, G.; Grimmer, M.; Seyfarth, A. The mechanisms and mechanical energy of human gait initiation from the lower-limb joint level perspective. Scientific Reports 2021, 11, 22473.

[20] Kolaghassi, R. Deep learning for gait prediction: an application to exoskeletons for children with neurological disorders. PhD thesis, University of Kent,, 2023.

[21] Cen, X.; Lu, Z.; Baker, J.S.; István, B.; Gu, Y. A comparative biomechanical analysis during planned and unplanned gait termination in individuals with different arch Stiffnesses. Applied Sciences 2021, 11, 1871.

[22] Park, T.G.; Kim, J.Y. Real-time prediction of walking state and percent of gait cycle for robotic prosthetic leg using artificial neural network. Intelligent Service Robotics 2022, 15, 527–536.

[23] Yen, Y.L.; Ye, S.K.; Liang, J.N.; Lee, Y.J. Recognition of walking directional intention employed ground reaction forces and center of pressure during gait initiation. Gait & Posture 2023, 106, 23–27.

[24] Baud, R.; Manzoori, A.R.; Ijspeert, A.; Bouri, M. Review of control strategies for lower-limb exoskeletons to assist gait. Journal of NeuroEngineering and Rehabilitation 2021, 18, 1–34.
[25] Zhang, M.; Zhu, Y.; Cao, A.; Wei, Q.; Liu, Q. Body trajectory optimisation of walking gait for a quadruped robot. IET Cyber-Systems and Robotics 2023, 5, e12094.
[26] Huang, L.; Zheng, J.; Hu, H. Online gait phase detection in complex environment based on distance and multi-sensors information fusion using inertial measurement units. International Journal of Social Robotics 2022, 14, 413–428.
[27] Kwon, C.W.; Yun, S.H.; Koo, D.K.; Kwon, J.W. Kinetic and Kinematic Analysis of Gait Termination: A Comparison between Planned and Unplanned Conditions. Applied Sciences 2023, 13, 7323.
[28] Laubscher, C.A.; Goo, A.C.; Sawicki, J.T. Optimal phase-based gait guidance control on a lower-limb exoskeleton. Control Engineering Practice 2023, 139, 105651.
[29] Zago, M.; Tarabini, M.; Delfino Spiga, M.; Ferrario, C.; Bertozzi, F.; Sforza, C.; Galli, M. Machine-learning based determination of gait events from foot-mounted inertial units. Sensors 2021, 21, 839.
[30] Abu-Faraj, Z.O.; Harris, G.F.; Smith, P.A.; Hassani, S. Human gait and clinical movement analysis. Wiley Encyclopedia of Electrical and Electronics Engineering 2015, pp. 1–34.
[31] Piming, G.; Yaming, Y.; Hai, S.; Xia, L.; Xiaobing, L. Three-dimensional ankle kinematics of the full gait cycle in patients with chronic ankle instability: A case-control study. Heliyon 2023, 9.
[32] Li, X.; Lu, Z.; Sun, D.; Xuan, R.; Zheng, Z.; Gu, Y. The influence of a shoe's heel-toe drop on gait parameters during the third trimester of pregnancy. Bioengineering 2022, 9, 241.
[33] Qin, S.; Chen, X.; Li, P.; Li, W.; Wu, Z.; Jiang, H.; Liu, Z.; Zhang, R. Modeling and evaluating full-cycle natural gait detection based on human electrostatic field. IEEE Transactions on Instrumentation and Measurement 2023.
[34] Sarshar, M.; Polturi, S.; Schega, L. Gait phase estimation by using LSTM in IMU-based gait analysis—Proof of concept. Sensors 2021, 21, 5749.
[35] Dong, Z.; Luces, J.V.S.; Ravankar, A.A.; Tafrishi, S.A.; Hirata, Y. A performance evaluation of overground gait training with a mobile body weight support system using wearable sensors. IEEE Sensors Journal 2023.
[36] Moll, F.; Kessel, A.; Bonetto, A.; Stresow, J.; Herten, M.; Dudda, M.; Adermann, J. Safety and Feasibility of Robot-assisted Gait Training in Adults with Cerebral Palsy in an Inpatient Setting–an Observational Study. Journal of developmental and physical disabilities 2023, pp. 1–16.
[37] Gurchiek, R.D.; Garabed, C.P.; McGinnis, R.S. Gait event detection using a thigh-worn accelerometer. Gait & posture 2020, 80, 214–216.
[38] Kim, G.T.; Lee, M.; Kim, Y.; Kong, K. Robust Gait Event Detection Based on the Kinematic Characteristics of a Single Lower Extremity. International Journal of Precision Engineering and Manufacturing 2023, pp. 1–14.
[39] Donahue, S.R.; Hahn, M.E. Estimation of gait events and kinetic waveforms with wearable sensors and machine learning when running in an unconstrained environment. Scientific Reports 2023, 13, 2339.
[40] Liu, Y.; Wu, J.; Qiu, X. Research on video emotion analysis algorithm based on deep learning. In Proceedings of the Basic & Clinical Pharmacology & Toxicology. Wiley 111 RIVER ST, HOBOKEN 07030-5774, NJ USA, 2021, Vol. 128, pp. 183–184.
[41] Huang, C.; Fukushi, K.; Wang, Z.; Nihey, F.; Kajitani, H.; Nakahara, K. An algorithm for real time minimum toe clearance estimation from signal of in-shoe motion sensor. In Proceedings of the 2021 43rd Annual International Conference of the IEEE Engineering in Medicine & Biology Society (EMBC). IEEE, 2021, pp. 6775–6778.
[42] Simpson, J.D.; Stewart, E.M.; Turner, A.J.; Macias, D.M.; Chander, H.; Knight, A.C. Lower limb joint kinetics during a side-cutting task in participants with or without chronic ankle instability. Journal of Athletic Training 2020, 55, 169–175.
[43] Racz, K.; Kiss, R.M. Marker displacement data filtering in gait analysis: A technical note. Biomedical Signal Processing and Control 2021, 70, 102974.
[44] Straczkiewicz, M.; Huang, E.J.; Onnela, J.P. A "one-size-fits-most" walking recognition method for smartphones, smartwatches, and wearable accelerometers. NPJ Digital Medicine 2023, 6, 29.
[45] Zhang, M.; Wang, Q.; Liu, D.; Zhao, B.; Tang, J.; Sun, J. Real-time gait phase recognition based on time domain features of multi-MEMS inertial sensors. IEEE Transactions on Instrumentation and Measurement 2021, 70, 1–12.
[46] Acosta-Sojo, Y.; Stirling, L. Individuals differ in muscle activation patterns during early adaptation to a powered ankle exoskeleton. Applied Ergonomics 2022, 98, 103593.
[47] Tudor-Locke, C.; Ducharme, S.W.; Aguiar, E.J.; Schuna, J.M.; Barreira, T.V.; Moore, C.C.; Chase, C.J.; Gould, Z.R.; Amalbert-Birriel, M.A.; Mora-Gonzalez, J.; et al. Walking cadence (steps/min) and intensity in 41 to 60-year-old adults: the CADENCE-adults study. International Journal of Behavioral Nutrition and Physical Activity 2020, 17, 1–10.
[48] Liu, Y.; Zhu, Q.; Cao, F.; Chen, J.; Lu, G. High-Resolution Remote Sensing Image Segmentation Framework Based on Attention Mechanism and Adaptive Weighting. ISPRS International Journal of Geo-Information 2021, 10. https://doi.org/10.3390/ijgi1004024 1.